Simulation of Sodium Dodecyl Sulfate at the Water−Vapor and Water−Carbon Tetrachloride Interfaces at Low Surface Coverage

Karl J. Schweighofer, Ulrich Essmann,† and Max Berkowitz*

Department of Chemistry CB3290, University of North Carolina, Chapel Hill, North Carolina 27599

Received: November 5, 1996[⊗]

To study the effect of the interface on the properties of an anionic surfactant molecule, sodium dodecyl sulfate (SDS), we performed two molecular dynamics computer simulations. In one simulation, the behavior of SDS at the water−vapor interface was examined. In parallel, we performed a simulation with the molecule embedded at the water−CCl_4 interface. A substantial difference in the configurational properties of the amphiphile was observed. At the water−vapor interface, the solute in its most probable configuration was bent, giving rise to two domains within the molecule: the first, containing the head group and several methyl groups, was solvated in water; the second, containing the rest of the molecule, lay down on the water surface. In contrast to these results, the molecule at the water−CCl_4 interface was straight on average, with a inclination of approximately 40° from the surface normal.

Introduction

The behavior of amphiphilic molecules at aqueous interfaces not only has long been of interest to those who study biological membranes but also has direct implications on processes such as vesicle formation, detergent action, lubrication, molecular self-assembly, foam stability, microemulsions, and ion-transfer, to name a few.[1] A large catalog of thermodynamic information on surfactants has been rendered from classical experimental techniques such as surface tension and surface potential measurements. Yet in order to have a full understanding of how these molecules behave, a molecular picture is required. Molecular dynamics of liquid interfaces has shown us the important effects that the molecular environment has on the behavior of solutes. Indeed, the interface is strongly responsive to the presence of certain solutes that can generate local disturbances that propagate far into the bulk.[2] Recent spectroscopic studies on surfactant monolayers at liquid−vapor[3] and liquid−liquid[4] interfaces have revealed molecular details that will enable us to move toward completing the picture, yet there are still many unanswered questions.

We are interested in one of the most common surfactants—the anionic detergent sodium dodecyl sulfate (SDS). SDS is probably one of the most widely used detergents and has many applications in industry and science. It is therefore of practical relevance to study the behavior of SDS at these interfaces.

There have been numerous experimental studies of monolayers at the water−vapor interface. One recent example is a comparative study of the different effects cationic and anionic surfactants have on interfacial water orientation using vibrational sum frequency generation (VSFG) on SDS and DDA (dodecylammonium) monolayers at the air−water interface.[3] There have also been several careful neutron reflection studies of monolayers containing SDS[5,6] and many more on other types of monolayers, such as those formed from the various C_nTAB class of surfactants.[7−10] In addition, a second harmonic generation (SHG) study on a compound related to SDS, the surfactant SNDS, or sodium 1-dodecylnaphthalene-4-sulfonate, compared the orientation of the surfactant molecules at the air−water, water−decane, and water−carbon tetrachloride interfaces.[11] Finally, VSFG studies of SDS at the water−carbon tetrachloride interface have recently been published,[4,12] resulting in information about the structure of the hydrocarbon tails, which was unobtainable from SHG studies.

On the theoretical side, a generalized van der Waals theory for nonuniform molecular fluids was used to characterize the adsorption and orientation of amphiphilic molecules at a model liquid−liquid interface.[13] There are also a number of molecular dynamics studies done on amphiphiles at water−vapor interfaces[14−17] and several on SDS micelles in bulk water.[18,19] We set forth in this study to compare the differences between systems containing SDS at the water−vapor and water−carbon tetrachloride interfaces in the limit of low surface coverage using molecular dynamics. This should allow a fairly comprehensive look at the effects of solvation on the amphiphile's orientational and conformational properties, as well as the structure of the fluids in the vicinity of the amphiphile.

TABLE 1: Na^+/Dodecyl Sulfate Intermolecular Potential Parameters

site	σ (Å)	ϵ (kcal/mol)	q
CH_3	3.905	0.175	0.000
CH_2 (internal)	3.905	0.118	0.000
CH_2 (attached to O)	3.905	0.118	0.137
O (ester)	3.000	0.170	−0.459
S	3.550	0.250	1.284
O (SO_3)	3.150	0.200	−0.654
Na^+	2.275	0.1153	1.000

Simulation Methodology

Simulation Parameters. Shown in Tables I−III are the parameters used in the simulations. The water model is SPC, with the bond lengths held constant through the use of the SHAKE algorithm.[20] The carbon tetrachloride is a fully flexible, nonpolarizable, five-site model. We have found that our model provides good agreement with a polarizable model of carbon tetrachloride[21] for the diffusion constant and also for static properties such as the density profile and radial distribution functions. The dodecyl sulfate hydrocarbon chain consists of a united atom CH_3 group connected to a hydrocarbon chain of 11 united atom CH_2 sites. The SO_4 group atoms are explicitly modeled. The dodecyl sulfate intermolecular and intramolecular potential parameters are also shown in the tables.

† Present address: GMD-SCAI, Schloss Birlinghoven 53754, Sankt Augustin, Germany.

⊗ Abstract published in *Advance ACS Abstracts,* April 1, 1997.

S1089-5647(96)03460-8 CCC: $14.00

TABLE 2: Dodecyl Sulfate Intramolecular Potential Parameters

group	K_{bend} (kcal mol^{-1} rad^{-2}), θ_0 (rad)	torsion[a]	K_{str} (kcal mol^{-1} Å^{-2}), R_0 (Å)
C−C−C	124.3, 111.0		
C−C−O(ester)	124.3,109.5		
C−O(ester)-S	124.3, 112.6		
O(ester)−S−O	102.0, 102.6		
O−S−O	102.0, 115.4		
C−C−C−C		R−B	
C−C−C−O(ester)		R−B	
C−C−O(ester)−S		R−B	
C−O−S−O		R−B	
C−C			620.0, 1.53
C−O(ester)			600.0, 1.42
O(ester)−S			600.0, 1.58
S−O			900.0, 1.46

[a] R−B = Ryckaert−Bellemans.

TABLE 3: CCl_4 Parameters[a]

site	σ (Å)	ϵ (kcal/mol)	q
C	3.410	0.100	−0.1616
Cl	3.450	0.285	0.0404

[a] $K_{Cl-C-Cl}$ = 149.0 (kcal mol^{-1} rad^{-2}), θ_0 = 109.5. K_{C-Cl} = 630.0 (kcal mol^{-1} Å^{-2}), R_0 = 1.766 (Å).

System Preparation and Equilibration. The water−CCl_4 system is comprised of 500 water and 222 carbon tetrachloride molecules in a rectangular box having X and Y dimensions of 24.834 Å and a Z dimension of 150.0 Å. The water−CCl_4 interface is in the XY plane at Z = 0 Å, with water occupying the left half of the box ($Z < 0$) and CCl_4 the right half ($Z > 0$). We define the interface location as the point along Z where the water density profile $\rho(Z)$ has half its bulk value and is in contact with the CCl_4. The box is longer in the Z direction than is needed to accommodate the two liquid slabs to prevent the formation of a second water−CCl_4 interface. Instead, there are two liquid−vapor interfaces at opposite ends of the box (on the $Z < 0$ side there will be a water−vapor interface and at the $Z > 0$ side, a CCl_4 liquid−vapor interface). These two liquid−vapor interfaces are not used to collect statistics. In addition, the Z dimension of the cell is chosen such that there is a very large separation between the liquid−vapor interfaces of the two liquids. It is also important to mention that both liquid−vapor interfaces are separated from the liquid−liquid interface by substantial regions of bulk liquid. Thus, there will be no direct effect on the water−CCl_4 interface from the liquid−vapor interfaces. The Z-dependent liquid density profiles of Figure 1 provide a visual description of how the system is put together.

The amphiphile was inserted into a fully equilibrated water−CCl_4 system such that the sulfur was located approximately in the center of the interfacial region with the hydrocarbon tail immersed in the organic layer and with an orientation slightly tilted relative to the interface normal. A random water molecule in the interfacial region was replaced by a sodium ion. The solvent−dodecyl sulfate interaction was turned on gradually over a period of 250 ps with periodic rescaling of the velocities to maintain a temperature of 300 K. This caused the least perturbation of the water−CCl_4 interface. The system was then equilibrated for another 500 ps using AMBER.[22] Since there are free charges in our system, we found it necessary to include a long-range electrostatic potential in the Hamiltonian. Long-range forces were calculated using Particle Mesh Ewald (PME)[23,24] with a potential cutoff radius of 9 Å for the Lennard-Jones interactions. The effects of the long-range forces on the interfaces is not yet known. However, we checked that equilibrium properties of this water−CCl_4 system do not differ qualitatively with those of other water−hydrocarbon systems in which long-range forces were absent.[25] The pure water−amphiphile system was created by taking the fully equilibrated water−CCl_4 system + SDS and removing the organic layer. The water located at the water−CCl_4 interface is the basis for a new water−vapor interface, where the SDS is adsorbed. The box length remained the same, and a 500 ps equilibration followed before production runs began. For both water−CCl_4 and water−vapor simulations, production runs used a time step of 1.0 fs and data collection every 20.0 fs for a total time of 1.0 ns.

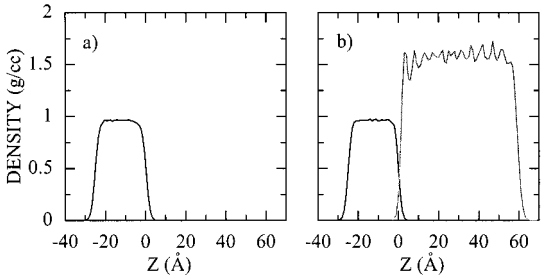

Figure 1. Liquid density profiles for the water−vapor system (a) and the water−CCl_4 system (b) obtained by dividing the simulation cell into 1 Å bins in the plane of the interface (XY plane). The location of the interface is defined as the point along the Z axis, where water has half its bulk value, and is at Z = 0.0 Å. Liquid−vapor regions at the extreme edges of the cell are not used to collect statistics.

Results

Liquid Density Profiles. The Z-dependent density distributions for the solvent in both the water−vapor and water−CCl_4 systems are shown in parts a and b of Figure 1, respectively. Both systems have liquid−vapor regions at the ends of the box with a vacuum space of about 20 Å between the liquid slabs. The dodecyl sulfate ion remains at the interface near Z = 0 Å for both systems. Oscillations in the carbon tetrachloride density distribution may be due in part to statistical fluctuations. Similar fluctuations have been seen in other liquid−liquid simulations.[25] The average bulk densities are 0.96 g/cm^3 and 1.59 g/cm^3 for water and carbon tetrachloride, respectively. The experimental densities at 300 K are 1.0 and 1.60 g/cm^3.

Head Group and Hydrocarbon Chain Locations. The large panels in parts a and b of Figure 2 show the Z-dependent atom-density distributions $\rho(Z)$ for the head and tail atoms of the amphiphile for the water−vapor and water−CCl_4 systems, respectively. Above these plots are shown the liquid density profiles for reference. Since we wish to compare our data with $\rho(Z)$ obtained from the neutron scattering of amphiphiles at the water−vapor interface, we define the regions of the amphiphile in the following way. The head group (hg) is defined as the SO_3^- group plus the Na^+ counterion. The hydrocarbon chain (hc) is defined as all united atom carbons from the methyl group to carbon 12. The carbon atoms are numbered starting from the methyl group (C1) and ending with the carbon atom (C12) that is attached to the esteric oxygen. The Z-dependent density profiles for the fragments are normalized such that the box cross-sectional area (L_xL_y) times the integral ($\int \rho(Z)\, dZ$) gives the number of atoms in the fragment. The point at which water has half its bulk density is at Z = 0 Å. In these figures the black-on-gray pair of lines shows the distribution of the hg fragment, the black line being a Gaussian fit to the distribution (in gray) using the formula

$$\rho = \rho_i \exp\left(\frac{-4(Z - Z_0)^2}{\sigma^2}\right) \quad (1)$$

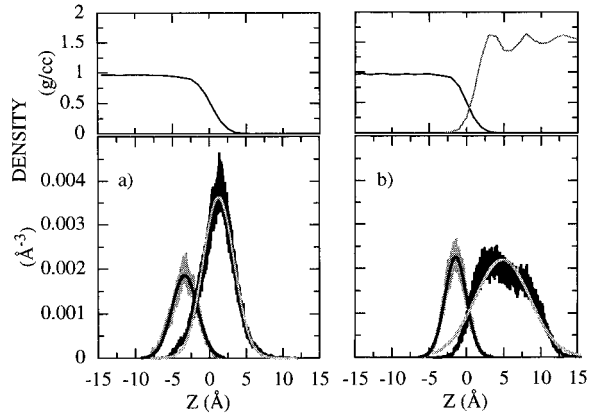

Figure 2. Atomic density profiles for the head group (hg) and hydrocarbon tail (hc) regions of the dodecyl sulfate amphiphile with the liquid density profiles for each system shown above for reference. The hg and hc regions are defined in the text. Panels a and b refer to the water−vapor and water−CCl_4 systems, respectively. In both panels, the smooth profiles are Gaussian fits superimposed on the original data, the leftmost curves referring to the hg and the rightmost curves referring to the hc regions.

TABLE 4: Centers (Z_0), 1/e Widths (σ), and Z Component of Head-Chain Separation (δ) for the Gaussian Distributions of Figure 2

	liq−vap	liq−liq
Z_0 (hg), Å	−3.37	−1.44
Z_0 (hc), Å	1.24	4.86
δ, Å	4.61	6.30
σ (hg), Å	4.92	4.09
σ (hc), Å	5.92	10.41

where ρ_i is the amplitude and Z_0 the center of the distribution. The gray-on-black curves refer to the hc fragment where the Gaussian fit is now represented by the gray line and the data is in black.

The Gaussian approximation appears to do quite well for the water−vapor case and for the hg distribution in the water−CCl_4 system. For the hc distribution, however, there are significant deviations from Gaussian. In this system, a pronounced bend developed in the center of the molecule, causing the methyl group to approach the interface in the early part of the trajectory. This caused a widening and distortion of the hc Z-dependent atom density distribution. This folded conformation was not preferable, and the molecule subsequently straightened out, remaining so for the rest ot the trajectory. A similar behavior was observed in simulations of an isolated dodecyl sulfate ion in bulk water.[18]

Table 4 shows the average positions (Z_0), widths (σ), and the Z component of the average head-to-chain separations (δ) based on these distributions. From the values for Z_0, we determine that the head group penetrates the water lamella by approximately 2.0 Å more in the water−vapor system than in the water−CCl_4 system. By examination of the profiles of Figure 2, it appears that part of the hc is solvated by the water at the vapor interface, whereas for the water−CCl_4 system the hc is predominantly solvated by the carbon tetrachloride. Experimental profiles for SDS at the water−vapor interface have not yet been published (to the authors' knowledge). However, in comparing our results to those obtained from neutron reflection studies on other types of monolayers, we conclude that low surface coverage and the relatively small size of the dodecyl sulfate head group allow penetration of the water−vapor interface to a greater extent than that seen for molecules with a larger head group or for monolayers that are more highly packed.

We now focus on the 1/e widths (σ) in Table 1 for the Gaussian distributions of Figure 2. For the water−vapor system the widths are 4.9 (hg) and 5.9 Å (hc), and for the water−CCl_4 system they are 4.1 (hg) and 10.4 Å (hc). The small value for the hc width for the water−vapor system is primarily due to the fact that the chain lies very close to the water surface on average, in contrast to the water−CCl_4 case where the chain has varying angles of tilt relative to the interface normal. Also, the position of the head group for the water−CCl_4 system seems to be more well defined than for the water−vapor system. The 1/e widths from the simulation may be related to those obtained from experiment after one approximates the contribution that surface roughness makes to the experimentally observed widths. It is now thought that a key contribution to this roughness comes from long wavelength capillary waves, which are excluded from the simulations by the presence of periodic boundary conditions. Therefore, the widths from simulations are generally going to be smaller than the experimental widths unless one corrects for this roughness. The experimentally observed width and "intrinsic" width of any fragment along the interface normal are assumed to be related through

$$\sigma_{obs}^2 = l^2 + w^2 \qquad (2)$$

where σ_{obs} is the experimentally observed width, l is the intrinsic width (actual width) of a fragment along the interface normal, and w is a measure of the roughness of the surface.[8] Factors contributing to the observed width are thermal fluctuations (capillary waves), mean tilt of the fragments with respect to the interface normal, and the incidence of gauche defects in the fragments.[26] To compare our widths with the experimentally observed widths obtained at very low surface coverages, we need to know w for our system. We have already mentioned that long wavelength capillary waves are excluded from the simulations, and these are a major contributor to w . Therefore, we need to obtain this parameter from the experiments. It is not possible to directly measure w. However, one can estimate it by making the simplifying assumption that the roughness is entirely attributable to capillary waves and can be obtained from the surface tension. An estimate of w for a C_{16}TAB monolayer with an area per molecule of 100 Å^2 gives 6.7 Å.[7] Assuming that a C_{16}TAB monolayer yields a similar value for the surface tension as would an SDS monolayer at the same surface coverage, we can use this value of w to correct our data. The corrected widths for the water−vapor system are 8.3 (hg) and 8.9 Å (hc), and for the water−CCl_4 system they are 7.8 (hg) and 12.4 Å (hc). Experimental widths are not yet available for SDS, but for $C_{12}E_3$ at a coverage of 89 Å^2/molecule on the water−vapor interface of water, σ_{obs}(hc) was approximately 12.0 Å.[26]

Amphiphile Single-Atom Distributions. Individual atom probability distributions $P(Z)$ for the dodecyl sulfate ion in the water−air and water−CCl_4 systems are shown in panels a and b of Figure 3, respectively. The thick lines to the right define the terminal methyl group distributions, whereas the thick lines on the left are the sulfur atom distributions. The thinner lines are for the other atoms in the dodecyl sulfate chain. The square graphs in panels c and d show the average of each distribution as a function of atom number (numbering starts from the methyl group C1 and goes toward the head region). Figure 3c refers to the water−vapor system, and Figure 3d refers to the water−CCl_4 system.

In comparing the distributions of parts a and b of Figure 3, one immediately notices that for the water−vapor system the distributions are much more compact along the Z axis, although their width suggests considerable motion out of the plane of

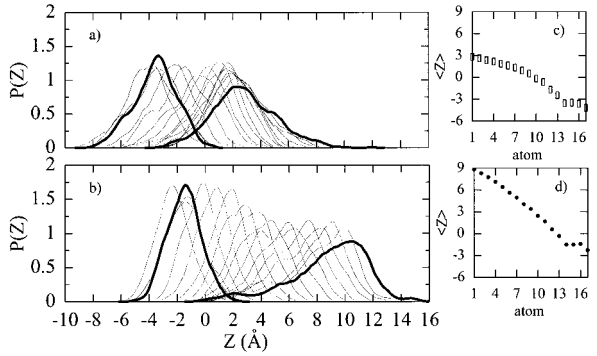

Figure 3. *Z*-dependent probability distributions for the individual sites in the dodecyl sulfate amphiphile. Panel a refers to the water−vapor system, whereas panel b refers to the water−CCl_4 system. The average of each distribution from panel a is shown in panel c. The average of each distribution from panel b is shown in panel d. The data shown in panels c and d reflect the average location of each site along the *Z*-axis (normal to the interface).

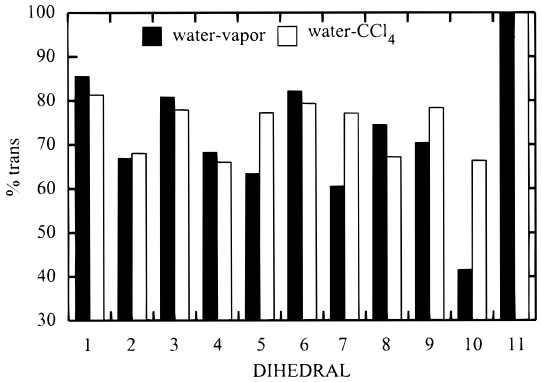

Figure 4. Trans statistics for the 11 dihedral angles in the backbone of the dodecyl sulfate amphiphile. Dihedral no. 1 refers to the endmost dihedral angle in which the terminal methyl group is a member. Dihedral no. 11 involves the sulfur atom and the three atomic sites behind it (in the direction of the methyl group) as explained in the text. The dark bars refer to the water−vapor system; the light bars refer to the water−CCl_4 system.

the interface. For the water−CCl_4 system, the distributions are more regularly spaced and do not penetrate the water surface (located at 0 Å) to the same degree as in the water−vapor system. In the water−vapor system, some of the carbons are actually immersed in the water. This is consistent with our view that part of the amphiphile is lying on the water−vapor surface a large percentage of the time. To maintain this configuration but still solvate the head group, the amphiphile must have a bend. We expect, therefore, an increased probability for gauche defects and bending of the chain near the head group region for the water−vapor case.

Evidence of the proposed bending of the molecule can be seen by examining the average position of each atom along the interface normal (parts c and d of Figure 3). For the water−vapor system shown in Figure 3c, the data are almost linear from C1 to C8 with a very gradual decrease in *Z* position as one progresses down the hydrocarbon chain from the tail toward the head. After C8 the atomic *Z* positions drop toward the water more for each successive step along the chain. Since variation in the average bond length between sites is very small, this signals the turning of the chain whereby atoms from C8 toward the head group orient more along the interface normal. This type of behavior has been seen in other simulations of amphiphilic molecules at the water−vapor interface at low coverage[14] and in experiments on dilute triethylene glycol monodecyl ether ($C_{12}E_3$) monolayers.[26]

For the water−CCl_4 system shown in Figure 3d, the average position of each site changes gradually with no noticeable breaks (except at site 14 where the sulfate oxygens adopt a tetrahedral arrangement around the sulfur). The *Z* component of the sulfur−methyl vector for this system can be measured to be 10.5 Å. The average length of the sulfur−methyl vector is 13.32 Å, indicating the molecule is, on average, tilted relative to the interface normal by approximately 40°.

Gauche defects may have an effect on the atom distributions above. Note that some of the distributions for the interior atoms are bimodal, suggesting there are two preferred positions along the *Z*-axis. This occurs most strongly in the water−CCl_4 system. However, one can also see shoulders in the C11 and C12 distributions for the water−vapor system. A change in conformation from gauche to trans (and back) near the head group may place tail atoms in two preferred positions along the *Z* coordinate. In a system with only one molecule, this type of motion would be less inhibited than for a densely packed monolayer. Preliminary results for monolayer systems of 36 dodecyl sulfate molecules at a surface coverage of 45 $Å^2$/molecule show this bimodality to be absent. Further analysis of the larger system (to be published forthcoming) will show whether this effect is statistical or results from the causes mentioned above.

Amphiphile Dihedral Distribution. The bar graph in Figure 4 shows the percentage of trans configurations for each dihedral in the hc fragment of the dodecyl sulfate anion. The black bars denote water−vapor and the light bars water−CCl_4 systems, respectively. The dihedral angles are numbered beginning with the $CH_3-CH_2-CH_2-CH_2$ fragment (C1−C2−C3−C4) and ending with the CH_2-CH_2-O-S fragment (C11−C12−O_{ester}−S). Figure 4 shows that the C11−C12−O−S dihedral (no. 11) is almost always trans (∼1% gauche). Two possible reasons for this are as follows: (1) a gauche conformation for this dihedral is sterically unfavorable, since it would bring the C11 atom in proximity to one of the anionic oxygens; (2) such a conformation would present the sulfur group as the leading atom and anionic oxygens facing away from the water. It would be more favorable to have the anionic oxygens available to the water so that they can participate in hydrogen bonding. Since simulation data suggest that water hydrogen bonding is enhanced at the water−vapor and water−hydrocarbon interfaces,[25,27] it is more favorable to incorporate the head group in a way consistent with minimal disruption of the hydrogen bond network.

Dihedral no. 10, on the other hand, exhibits a large proportion of gauche defects. This effect is strongest in the water−vapor system where the no. 10 dihedral has only 40% trans character. This has important consequences. For the water−CCl_4 system, flipping from gauche to trans at dihedral no. 10 may contribute to the bimodal character discussed in the last section and may also contribute to the overall tilt of the molecule with respect to the interface normal. For the water−vapor system, it may lead to the reorientation of the molecule's tail region so that it lies on the water surface. Such reorientation, however, can only occur in conjunction with subsequent gauche defects further along the chain. The two most likely candidates for defect sites are dihedral nos. 7 and 5. These sites show a marked decrease in % trans configurations over the water−CCl_4 system. Evidence to support that this is responsible for the orientation of the tail in the water−vapor system comes from the analysis in the last section of the average atom distributions of Figure 3c, where it was suggested that in the vicinity of C8 a discontinuity appears, which suggests reorientation of the tail section of the molecule.

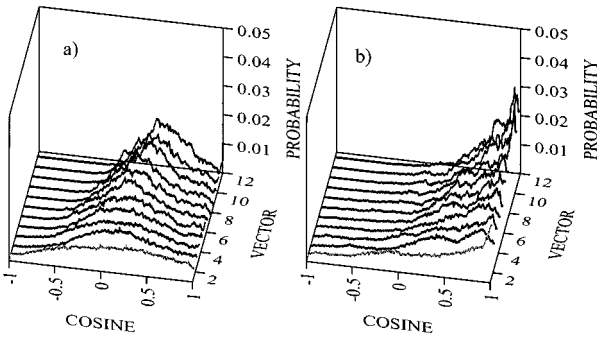

Figure 5. Probability distributions for the cosine of the angle between the interface normal and the vectors $\mathbf{R}_{ij}$ defined in the text. Panels a and b refer to the water−vapor and water−CCl_4 systems, respectively. The light-colored line in each plot gives the distribution of angles sampled by the CH_2-CH_3 bond vector.

Thus, although the overall number of gauche defects in both systems is similar (28% water−air vs 24% water−CCl_4), their distributions along the chain are different. In the water−vapor system where these defects are more concentrated on several sites, they lead to a predominant molecular orientation, whereas in the water−CCl_4 system they behave more like random perturbations.

Amphiphile Orientation. Figure 5 shows the distributions of the orientational cosines defined by

$$\cos(\theta) = \mathbf{z}\cdot\frac{\vec{R}_{1j}}{|\vec{R}_{1j}|} \qquad (3)$$

where $\vec{R}_{1j}$ refers to the $\vec{R}_{\text{methyl}} - \vec{R}_j$ vector, $j = \{2,3,4, ..., 12\}$, and $\mathbf{z}$ is the unit vector in the Z-direction. In the plots, the vectors are labeled by their j values. These vectors all point in the direction toward the methyl group, and carbon 12 is the atom adjacent to the ester oxygen. Note that $\vec{R}_{1,2}$ is the CH_3-CH_2 terminal bond vector.

Figure 5a shows that for the water−vapor system, the terminal bond vector ($j = 2$) is very broadly distributed with no obvious preferred orientation. The rest of the distributions are centered approximately around zero but with a slight shift toward 1.0 as j increases. This indicates that the orientations in the plane of the interface are preferred. For the water−CCl_4 system (Figure 5b) all distributions are much more strongly biased toward the interface normal compared to the water−vapor system. If we use the vector $\vec{R}_{1,12}$ to describe the orientation of the tail region, we find the average angle that $\vec{R}_{1,12}$ makes with the interface normal is approximately 42°. This is in agreement with our estimate of 40° for the tilt angle using the atom distributions of Figure 3 for the water−CCl_4 system. Preferential orientation toward the interface normal for dodecyl sulfate at the water−CCl_4 interface has recently been observed experimentally.[4]

Head Group−Water Radial Distribution Functions. Head group−water radial distribution functions for the water−vapor system are shown in Figure 6. Four types of correlations were calculated: $g(r_{\text{o-wo}})$, $g(r_{\text{o-wh}})$, $g(r_{\text{s-wo}})$, and $g(r_{\text{s-wh}})$. The first two refer to the correlations between an anionic sulfate oxygen on the dodecyl sulfate ion and the water oxygen (wo) or water hydrogen (wh). The second two refer to the correlations between the sulfur atom and the water. The panels are divided such that correlations involving a water oxygen atom are shown in panel a, whereas those involving a water hydrogen are shown in panel b. Within each panel, dotted lines indicate anionic sulfate oxygen−water correlations. Solid lines depict sulfur−water correlations. The hg−water radial distribution functions

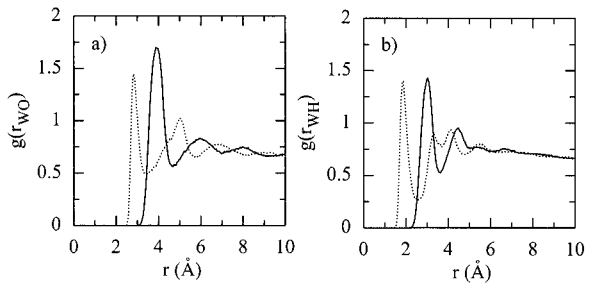

Figure 6. Head group−water radial distribution functions. Panel a shows correlations involving the oxygen atoms of water. Panel b shows correlations involving the water hydrogen atoms. The $g(r)$ depicted with dotted lines have origins placed on the anionic oxygens of the sulfate group. Solid lines refer to $g(r)$ calculated with the sulfur atom as the origin. Both panels are for the water−vapor system.

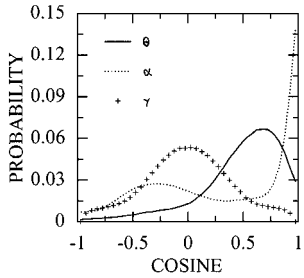

Figure 7. Orientational distribution functions for water in the first solvation shell of the head group. θ refers to the angle between the S−H_2O vector and the water dipole. α refers to the angle between the S−H_2O vector and the OH bond. γ refers to the angle between the S−H_2O vector and the normal to the H−O−H plane.

were also calculated for the water−CCl_4 system and found to differ negligibly from the water−vapor results, suggesting the aqueous environment of the head group is conserved between the two systems. For this reason we only show the results for the water−vapor system.

It is important to mention first that the radial distribution functions are normalized to the bulk density of water. Therefore, they will decay to a value less than 1.0 at large distances, since the solute is located in the interfacial region where the density of water is less than it is in bulk. This way of calculating $g(r)$ compares the number of neighbors around a solute site to the number expected if it were immersed in an homogeneous medium. From the solid line in Figure 6a, $g_{\text{s-wo}}$ shows a peak at 4.0 Å and a second solvation shell near 6.0 Å. The first minimum occurs at approximately 4.8 Å, and all water oxygens within this solvation sphere are first-shell water molecules. In the Figure 6b (solid line) $g_{\text{s-wh}}$ has a first peak centered close to 3.0 Å, which means that the hydrogen is closer to the sulfur atom by about 1.0 Å. This indicates that the orientation of water around the head group is with the water hydrogen pointing toward the sulfur. The functions $g_{\text{o-wo}}$ (dotted line, Figure 6a) and $g_{\text{o-wh}}$ (dotted line, Figure 6b) show that the hydrogen of water is on average 1.9 Å away from the sulfate oxygen, whereas the sulfate oxygen−water oxygen distance is about 2.9 Å. This is close enough for the water surrounding the sulfate group to hydrogen bond to the head group with one hydrogen and still participate in hydrogen bonding with neighboring water molecules.

Water Orientation around the Head Group. The water orientational distributions for water in the first solvation shell of the head group for the water−vapor system are shown in Figure 7. The first solvation shell was defined by the sulfur−water oxygen radial distribution functions as discussed above. Again, the water−CCl_4 results are very similar and are not

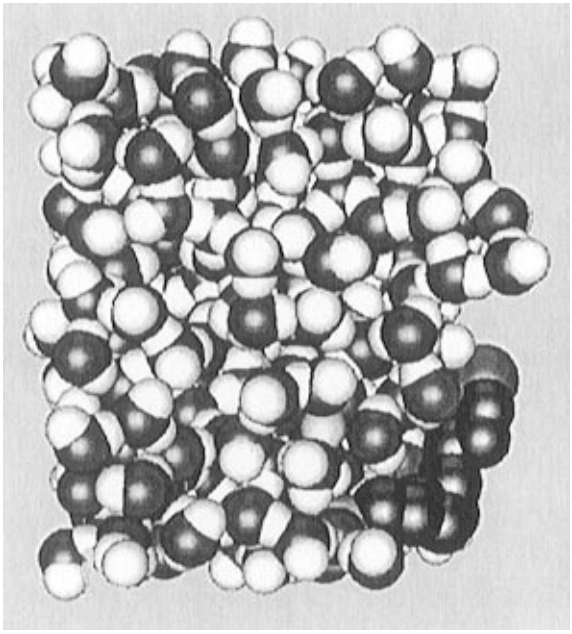

Figure 8. Instantaneous configuration for the dodecyl sulfate anion at the water−vapor interface. Only atoms in the interfacial region are shown. Part of the head group of the amphiphile is obscured by water molecules. The larger gray sphere adjacent to the last CH_2 group is the terminal methyl group of the amphiphile.

shown. Three orientational cosines are presented. The angle θ is defined by the water dipole vector and the water oxygen-to-sulfur vector. α is the angle between the water OH bond vector and the water oxygen-to-sulfur vector. Last, γ is the angle between the vector normal to the water H−O−H plane and the water oxygen-to-sulfur vector.

The θ distribution is rather broad but indicates that on average the water dipole is pointing approximately 50° away from the oxygen-to-sulfur vector. This should place one of the water hydrogens pointing toward the sulfur group. This is confirmed by the distribution for α, which is bimodal and has preferred orientations of 109° and 0°, as expected, since the H−O−H angle is constrained to be 109.5° and one of the water OH bonds lines up with the oxygen-to-sulfur vector. The third angle, γ, is broadly centered about 90°. Thus, if a water OH bond points to the sulfur group, then the other water OH bond rotates around the line containing the O−H−S atoms. This orientation is expected, since the water hydrogens will attempt to hydrogen bond with the negatively charged sulfate oxygens. This type of orientation was also suggested from the radial distribution functions above.

Experimentally, it is found that for monolayers of charged surfactants on an water−vapor interface, water molecules in the interfacial region orient in response to the charged layer.[3] In this case, the system behaves as if it were in the presence of a charged electrode surface. The effect that we are observing at low surface coverage, however, is a more subtle effect, involving only the small number of water molecules that are present in the solvation shell of the charged head group. The orienting of water is therefore a local effect and is similar to that observed for an SO_4^{2-} anion simulated in bulk water.[28]

Representative "Snapshots". Figures 8 and 9 show representative configurations of the amphiphile at the water−vapor and water−CCl_4 interfaces, respectively. Figure 8 shows clearly the bending of the hc as a result of gauche defects mentioned in the previous sections. In both figures, the polar hg regions are well solvated by water. Figure 9, in addition, has captured a gauche defect several sites away from the methyl group. Such defects are common.

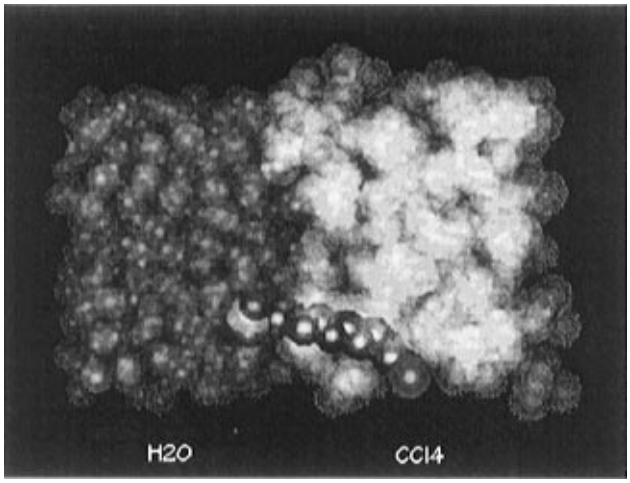

Figure 9. Instantaneous configuration for the dodecyl sulfate anion at the water−CCl_4 interface. Only atoms in the interfacial region are shown. The solvent molecules are drawn as translucent spheres, with white spheres representing CCl_4 molecules and gray spheres representing water oxygen atoms (water hydrogens are not shown for clarity). The amphiphile can clearly be seen with its head group in the water phase and its tail region in the nonpolar phase.

Discussion

We have presented a molecular picture of the surfactant sodium dodecyl sulfate at the water−vapor and water−carbon tetrachloride interfaces. We have shown that the preferred orientation of the molecule at low surface coverage is different in the two systems. The water−vapor interface provides an attractive surface for the molecule's hydrocarbon tail to lay on, and in the absence of interactions with a nonpolar solvent or hydrocarbon tails from neighboring molecules, the amphiphile will adopt a bent conformation. This allows the head group region to insert into the aqueous phase and achieve maximum solvation while the tail maximized its van der Waals interactions with the surface water. Gauche defects concentrated at certain locations along the chain make this conformation possible. This behavior is supported by a model based on neutron reflection data of triethylene glycol monodecyl ether adsorbed on the water−vapor interface.[26] A previous molecular dynamics simulation of a model amphiphile at the water−vapor interface also supports these findings.[15] For this model amphiphile, it was found that the head group tries to insert into the water nearly perpendicular to the plane of the interface while the tail lies close to the surface.

When the tail region is solvated by carbon tetrachloride, the molecule adopts a tilted orientation relative to the surface normal. The molecular orientation is biased toward the interface normal. The incidence of gauche defects is slightly less than in the absence of the nonpolar liquid, but only by a small amount. These defects however, do not appear to result in any strong or persistent bends in the molecule.

In comparing the behavior of SDS between the two interfacial systems, we have illustrated the effects on orientation that result from the subtle balance of forces due to van der Waals, dihedral, and thermal (entropic) contributions. For the water−vapor system, the van der Waals attraction of the tail to the water surface plays the major role in determining the overall molecular orientation and conformation. In part, this is due to the fact that the total number of gauche defects does not have to be increased by a large amount to make the molecule lay down on the water surface. The distribution of defects clearly emphasizes certain sites, allowing the molecule a "bending region" (in our

example, the region near C7 and C8). Still, the orientational profiles are broadened considerably by the thermal factors that attempt to randomize the chain. For the water−CCl_4 system, the van der Waals interaction between the SDS and the solvent is rather uniform throughout the system given that, on average, the SDS remains pointing into the CCl_4. The tendency for the dihedral interaction to favor trans conformations prevents the SDS from remaining bent, though it still allows some defects to increase entropy. In the future we will examine monolayers of SDS at these interfaces so that we can ascertain the effects of the tail−tail interactions on molecular orientation and conformation. Our preliminary results indicate that these play a major role in determining the amphiphile orientation in denser monolayers.

Acknowledgment. The authors thank Michel Crowley at the Pittsburgh Supercomputer Center for a preliminary version of the AMBER/PME code, Tom Darden and Lalith Perera for helpful discussions, and the reviewers for their instructive comments. K.J.S. also thanks Ilan Benjamin for suggestions concerning the manuscript. These calculations were performed at the North Carolina Supercomputer Center on the Cray T3D and through a grant from the Office of Naval Research.

References and Notes

(1) See, for example, the following. *Prog. Colloid Polym. Sci.* **1995**, *100*, and references contained therein. Gelbart, W. M.; Ben-Shaul, A. *J. Phys. Chem.* **1996**, *100*, 13169−13189.

(2) Benjamin, I. *Science* **1993**, *261*, 1558−1560.

(3) Gragson, D. E.; McCarty, B. M.; Richmond, G. L. *J. Phys. Chem.* **1996**, *100*, 14272−14275.

(4) Conboy, J. C.; Messmer, M. C.; Richmond, G. *J. Phys. Chem.* **1996**, *100*, 7617−7622.

(5) Lu, J. R.; Marrocco, A.; Su, T. J.; Thomas, R. K.; Penfold, J. *J. Colloid Interface Sci.* **1993**, *158*, 303−316.

(6) Purcell, I. P.; Thomas, R. K.; Penfold, J.; Howe, A. M. *Colloids Surf. A* **1995**, *94*, 125−130.

(7) Lu, J. R.; Hromadova, M.; Thomas, R. K.; Penfold, J. *J. Phys. Chem.* **1994**, *98*, 11519−11526.

(8) Lu, J. R.; Hromadova, M.; Thomas, R. K.; Penfold, J. *J. Chem. Soc., Faraday Trans.* **1996**, *92*, 403−408.

(9) Simister, E. A.; Thomas, R. K.; Penfold, J.; Aveyard, R.; Binks, B. P.; Cooper, P.; Fletcher, P. D. I.; Lu, J. R.; Solokowski, A. *J. Phys. Chem.* **1992**, *96*, 1383−1388.

(10) Simister, E. A.; Lee, E. M.; Thomas, R. K.; Penfold, J. *J. Phys. Chem.* **1992**, *96*, 1373−1382.

(11) Grubb, S. G.; Kim, M. W.; Raising, T.; Shen, Y. R. *Langmuir* **1988**, *4*, 452.

(12) Messmer, M.; Conboy, J. C.; Richmond, G. *J. Am. Chem. Soc.* **1995**, *117*, 8039−8040.

(13) Telo da Gama, M.; Gubbins, K. E. *Mol. Phys.* **1986**, *59*, 227.

(14) Pohorille, A.; Benjamin, I. *J. Chem. Phys.* **1991**, *94*, 5599.

(15) Pohorille, A.; Benjamin, I. *J. Phys. Chem.* **1993**, *97*, 2664.

(16) Tarek, M.; Tobias, D. J.; Klein, M. L. *J. Phys. Chem.* **1995**, *99*, 1393−1402.

(17) Bocker, J.; Schlenkrich, M.; Bopp, P.; Brickmann, J. *J. Phys. Chem.* **1992**, *96*, 9915−9922.

(18) Shelley, J.; Watanabe, K.; Klein, M. L. *Int. J. Quantum Chem.* **1990**, *S17*, 103−117.

(19) MacKerell, A. D. *J. Phys. Chem.* **1995**, *99*, 1846−1855.

(20) Ciccotti, G.; Ryckaert, J. P. *Comput. Phys. Rep.* **1986**, *4*, 345.

(21) Chang, T.-M.; Peterson, K. A.; Dang, L. *J. Chem. Phys.* **1995**, *103*, 7502−7513.

(22) Weiner, S. J.; Kollman, P. A.; Nguyen, D. T.; Case, D. A. *J. Comput. Chem.* **1986**, *7*, 230.

(23) Darden, T. A.; York, D. M.; Pedersen, L. G. *J. Chem. Phys.* **1993**, *98*, 10089−10092.

(24) Essmann, U.; Perera, L.; Berkowitz, M. L.; Darden, T.; Lee, H.; Pedersen, L. G. *J. Chem. Phys.* **1995**, *103*, 8577−8593.

(25) Benjamin, I. *J. Chem. Phys.* **1992**, *97*, 1432.

(26) Lu, J. R.; Hromadova, M.; Thomas, R. K.; Penfold, J. *Langmuir* **1993**, *9*, 2417−2425.

(27) Schweighofer, K. J.; Benjamin, I. *J. Electroanal. Chem.* **1995**, *391*, 1−10.

(28) Cannon, W. R.; Pettitt, B. M.; McCammon, J. A. *J. Phys. Chem.* **1994**, *98*, 6225−6230.